Interplay between tip-induced band bending and voltage-dependent surface corrugation on GaAs(110) surfaces

G. J. de Raad, D. M. Bruls, P. M. Koenraad, and J. H. Wolter
COBRA Inter-University Research Institute, Eindhoven University of Technology, P.O. Box 513, 5600 MB Eindhoven, The Netherlands
(Received 9 October 2001; revised manuscript received 29 May 2002; published 6 November 2002)

Atomically resolved, voltage-dependent scanning tunneling microscopy (STM) images of GaAs(110) are compared to the results of a one-dimensional model used to calculate the amount of tip-induced band bending for a tunneling junction between a metal and a semiconductor. The voltage-dependent changes in the morphology of the atomic lattice are caused by the four surface states of the GaAs(110) surface contributing in varying relative amounts to the total tunneling current. Tip-induced band bending determines which of these states contributes to the total tunneling current at a given bias voltage, and thus has a profound influence on the voltage-dependent STM-images. It is shown that certain voltage regions exist, for which none of the surface states present at the GaAs(110) surface can contribute to the tunneling current. For these voltages, tunneling occurs between the tip and bulk states of the sample through a surface depletion layer several nm wide. Nevertheless, we observe atomic, surface like corrugation for these circumstances.

DOI: 10.1103/PhysRevB.66.195306 PACS number(s): 68.37.Ef, 71.55.Eq, 73.20.At

I. INTRODUCTION

As was shown by Ebert *et al.*[1] for GaAs, GaP, and InP, the apparent direction of the atomic rows on the {110} surfaces of these materials can change from the $[-110]$ direction to the $[001]$ direction as a function of applied bias voltage, when imaged by atomically resolved scanning tunneling microscopy (STM). The {110} surface of these semiconductors is made up of zigzag rows of alternating anions and cations extending along $[-110]$ [Fig. 1(a)]. It was shown that the apparent direction of the atomic rows is governed by different surface states contributing in varying relative amounts to the total tunneling current [see Fig. 1(c)]. These states have a different location and spatial extent within the surface unit cell. When the relative contributions of these states to the total tunneling current change, so too does the appearance of the surface in atomically resolved STM.

In the energetic range accessible to STM, the surface-density of states (DOS) of the {110} surfaces of GaAs, InP, and GaP is dominated by four states designated $A5$, $A4$, $C3$ and $C4$.[1–3] The energies that Ebert *et al.* calculate for these surface states for the relaxed, free InP {110}-surface are listed in Table I.[1] These same states with similar energetic location are also found on GaAs {110}.[2] The surface DOS of InP has later been described in great detail by Engels *et al.*[3] The $A5$ and $A4$ states are both localized on the anions and extend along $[-110]$. The $A5$ state has a dangling bond character and the $A4$ state is a back-bond state.[1,3] The $C3$ state is localized on the cations, extends along $[001]$[1,3] and is an empty dangling-bond state with p_z character.[3] The state commonly designated as $C4$ in reality consists of several empty surface resonances with different spatial extent and slightly different energetic location.[3] Close to the surface ($2.23a_0 = 1.1$ Å from the outwardly rotated P atoms), the $C4$ state is localized on both the cations and anions and appears as a zigzag row. Further away from the surface ($6.53a_0$ from the surface anion) the state shows as maxima centered on the cations extending along $[-110]$.[1,3] References 1 and 3 also show that if both the $C3$ and $C4$ states contribute to the tunneling current, the $C4$ state will dominate in the STM image. Consequently, the atomic rows will appear to run along $[001]$ if the contribution from the $C3$ state dominates the tunneling current. If any of the other states dominates, the rows will appear to run along $[-110]$ (also see Fig. 1 and Table I). In intermediate cases, the image will show clear atomic corrugation in both directions.

It is also important to note that, although no surface state on the GaAs {110} is centered inside the bulk band gap, the shoulder of the unoccupied surface states *does* extend into the band gap.[3,4] In Ref. 4 it is noted that the bottom of the ''empty cation derived surface band'' has its localization along the $\langle 001 \rangle$ bulk direction. It is also shown that the onset of this surface band lies well inside the bandgap. Most of the charge density associated with this band lies within the surface layer.[4] Reference 3 indicates for InP {110} that at $6.53a_0$ (3.3Å) from the relaxed anions, the local DOS associated with the unoccupied surface states ($C3$ and $C4$) vanishes near the conduction-band maximum (CBM), implying that the part of the $C3$-state that extends into the bandgap decays rapidly into the vacuum.

For a surface state to contribute to the total tunneling current, it has to lie energetically between the tip Fermi level (TFL) and the sample Fermi level (SFL) [see Fig. 1(d)]. Whether a given surface state lies inside this energetic window depends not only on the applied bias voltage, but also on the amount of tip-induced band bending (TIBB). The influence of TIBB was already demonstrated qualitatively in Ref. 5, whose authors observed local changes in corrugation around Ag nano-clusters deposited on a GaAs {110} surface. In order to understand the voltage-dependent changes in atomically resolved STM images of GaAs{110}, knowledge of the electronic structure of the surface and information about the amount of TIBB as a function of applied bias voltage, are both essential. Moreover, TIBB can cause tunneling to occur between the tip and bulk states of the sample through a surface depletion layer.[6] In spite of this, recent

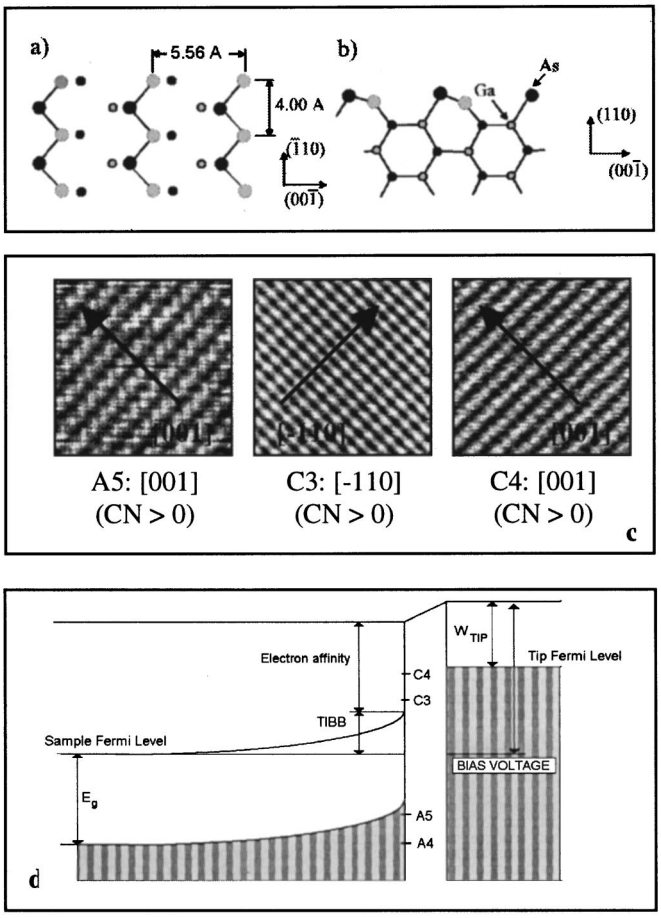

FIG. 1. (a) Relaxed GaAs(110) surface (top view). (b) Side view. (c) Direction of corrugation and sign of the corrugation number (CN) for the *A*5, *C*3, and *C*4 states. Notice that the direction of corrugation is perpendicular to the apparent direction of the atomic rows. The STM images are rotated by 45° with respect to the sketch in (a). (d) Energetic location of the *A*4, *A*5, *C*3, and *C*4 states. The effect of Tip-induced band bending (TIBB) is also sketched in the diagram.

literature on voltage-dependent changes in STM images of GaAs {110} considers TIBB only in qualitative terms.[1,3,7]

In this paper we compare voltage-dependent STM images of *n*-type and *p*-type GaAs {110} to the results of a one-dimensional model that calculates the amount of TIBB as a function of bias voltage. The study involves both polarities of the bias voltage. We will show that the observed changes in the atomic corrugation are consistent with the band-bending behavior that the model predicts.

Furthermore, we observe a very interesting phenomenon: When *p*-type GaAs is imaged at small negative sample bias ($V=-0.5$ V), the electrons tunnel from the valence-band states in the bulk of the sample, through a surface depletion layer to the tip. This mode of tunneling has been described in Ref. 6, and one of its characteristics is that due to band bending, none of the four surface states is energetically available to the tunneling process. In spite of that, for these circumstances we observe atomic corrugation with the same periodicity as the surface lattice. We will show that the changes in atomic corrugation observed in the filled-state

TABLE I. Some properties of the four surface states on the {110} surfaces of GaAs and InP that are accessible to STM. The band gap has been listed as well to facilitate the reader. The energies of the surface states have been calculated for the relaxed InP {110} surface (Refs. 1 and 3).

Surface state	Energy for relaxed InP {110}[1] (VBM=0 eV)	Direction of corrugation	Centered on
*C*4	+2.27 eV to +2.81 eV	[001]	cations
*C*3	0 eV to +2.27 eV	[−110]	cations
Fundametal bandgap (InP) (Ref. 13)		0–1.35 eV	
*A*5	0 eV to −0.95 eV	[001]	anions
*A*4	−0.95 eV to −1.77 eV	[001]	anions

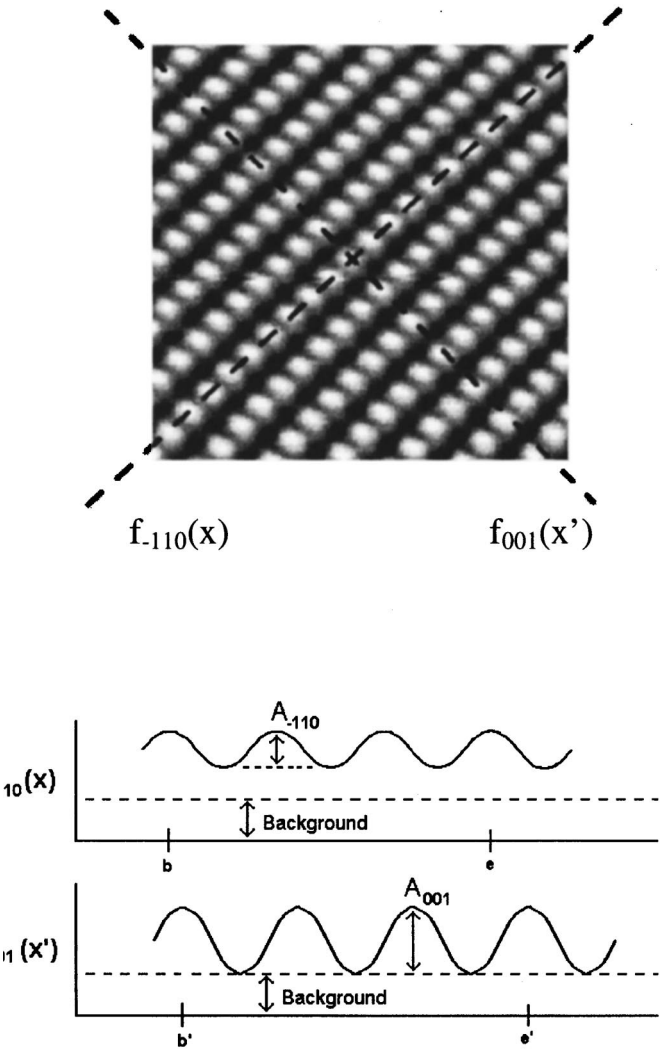

FIG. 2. (a) Position of the line profiles used for calculating the CN. The line profiles always pass through the atomic maxima in the image. (b) Sketch of the resulting line profiles. In this example, the CN is positive (CN>0). See further details in the text.

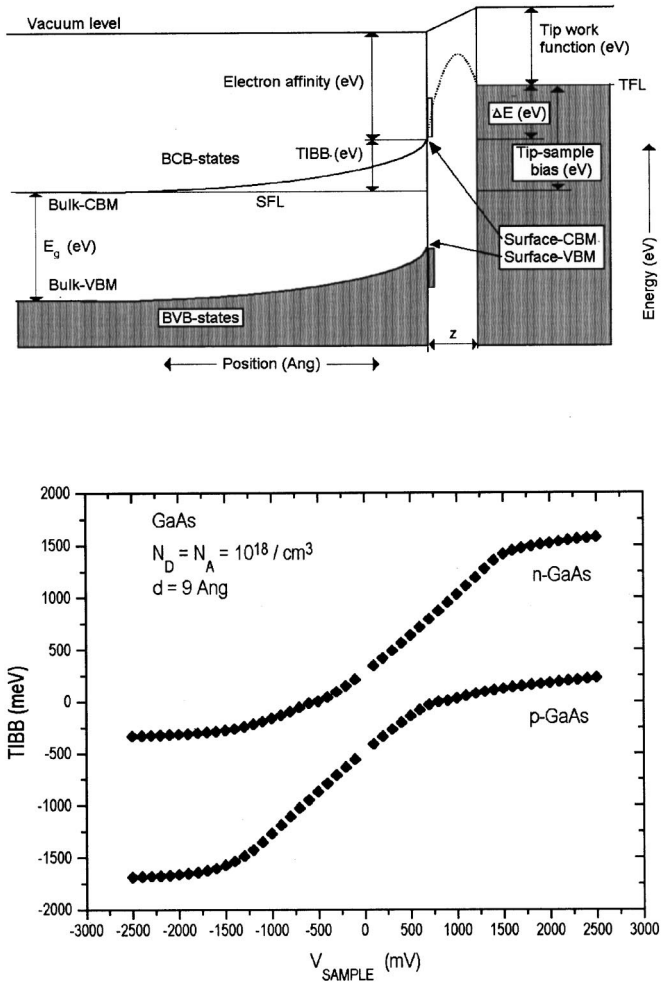

FIG. 3. (a) Definition of the various constants used in the model. The dotted line indicates the potential inside the vacuum barrier when the image charge is taken into account. This is the potential barrier used to calculate the tunneling current. The two bands of surface states are indicated by the rectangles near the surface. CBM and surface VBM. (b) Calculated TIBB for *n*-GaAs and *p*-GaAs for a fixed tip-sample distance (9 Å). The tip work function (W_{TIP}) is 4.6 eV.

images of *p*-GaAs can only be explained in a manner that is consistent with the band bending model when it is assumed that the current of electrons tunneling from the bulk states to the tip is spatially modulated so as to produce an atomic like corrugation in the STM image. This mechanism for atomic corrugation does not involve electrons tunneling directly into or out of surface states, which is the common way to understand atomic corrugation in STM images of semiconductor surfaces. We hypothesize that this alternative mechanism for atomic corrugation is caused by atomic-scale variations of the tunneling barrier-height[8,9] or by a site-dependent tip-sample interaction.

II. EXPERIMENT

The STM work was performed in ultrahigh vacuum (OMICRON STM-1 setup operated at 4×10^{-11} torr) on *in situ* cleaved GaAs samples. Doping concentrations were 10^{18}-cm^{-3} Si for *n*-doped material (*n*-doped substrate[10]) and 10^{18}-cm^{-3} Be for *p*-doped material (a 1-μm-thick molecular beam-epitaxy-grown layer on *p*-doped substrate). Our tips are etched electrochemically from 0.25-mm-polycrystalline tungsten wire. After heating, Ne^+-ion self-sputtering and bombardment by an Ar^+ ion gun, our tips routinely yield atomic resolution on GaAs/InP(110) (apex radius $\sim$10 nm).[11] The bias voltage is applied to the sample. Our STM setup is equipped with a ''dual mode'' feature, which enables us to apply one set of scan parameters (bias voltage, tunneling current, and feedback parameter) on the forward scan and another set of parameters on the backward one. We can thus image a given area of the sample simultaneously for two different sets of parameters. All images shown in this paper are height images $[z(x,y)]$ that were obtained while operating the STM in a constant-current mode.

Changes in the atomic corrugation are commonly expressed as the ratio of corrugation amplitudes along the $[-110]$ and $[001]$ directions.[1] We deviate from that. Our ''corrugation number'' (CN) is calculated from two line profiles, which are taken along $[-110]$ and $[001]$, respectively, and which both pass through the atomic maxima of the image [$f_{-110}(x)$ and $f_{001}(x')$, see Fig. 2(a)]. Before we take the line profiles, we apply the usual ''tilt'' background correction to the image, followed by the ''line-by-line tilt correction'' described in Ref. 12. We then calculate the average height along both profiles (H_{-110} and H_{001}). The begin and end points of the integrals (b,e,b',e') are always chosen at an atomic maximum in the image. Notice that using the difference in average height cancels out any possible background term. The difference in average height is divided by the corrugation amplitude along either $[-110]$ or $[001]$, whichever is largest $[\max(A_{-110},A_{001})]$. The resulting CN lies between -0.5 and 0.5, corresponding to a corrugation appearing as straight, parallel lines along $[-110]$ for a CN of $+0.5$, and to one appearing as straight, parallel lines along $[001]$ for a CN of -0.5. A CN close to zero corresponds to a clearly resolved atomic corrugation in both directions [see Fig. 1(c) for examples]. Mathematically the CN is defined as

$$\mathrm{CN}=\frac{H_{-110}-H_{001}}{\max(A_{-110},A_{001})}, \tag{1}$$

with

$$H_{-110}=\frac{\int_b^e f_{-110}(x)dx}{e-b} \quad \text{and} \quad H_{001}=\frac{\int_{b'}^{e'} f_{001}(x')dx'}{e'-b'}. \tag{2}$$

During high-resolution STM, tip changes which alter the appearance of the atomically resolved lattice are a common occurrence. Such changes are easily recognized as a sudden and spontaneous change in apparent corrugation and tip-sample separation. If during the acquisition of a series of voltage-dependent images (one column in Fig. 5) a tip-change is observed to irreversibly change the corrugation, we only compare those images that were recorded either *before* or *after* the tip change in order to ensure that only those

images are compared that were recorded while the tip had the same tip DOS. Another way to verify that the changes in atomic morphology are not influenced by a change in the tip DOS during the measurement is to record a reference image at some fixed voltage at regular intervals during the measurement, or on the backward leg of the tip motion while operating the STM in a dual mode. A tip change will manifest itself as a change in the reference image. In practice, tip changes do not present much of a problem. Our tips usually yield stable and reproducible images throughout most of the intended voltage region ($0.5\ \mathrm{V} < V < 2.5\ \mathrm{V}$ of either polarity). Most of the tip changes occur near the extrema of this voltage range where either the tip-sample distance becomes small or the electric field between the tip and sample becomes large. If a tip is observed to yield unstable images, it is exchanged for another one. In most cases, a tip-change causes a (slight) shift in the voltage at which the change in atomic corrugation occurs. The general trends usually remain the same.

As an aid in the interpretation of the results, we also use a one-dimensional model to describe band bending for a tunneling junction between a metal tip and a GaAs {110} surface. Apart from the addition of two bands of surface-states, the model is equivalent to the model presented in Ref. 6. The main input parameters are the bias voltage (V), the tip-sample distance (z), the tip work function (W_{TIP}), the sample surface electron affinity [$\chi = 4.07$ eV for GaAs (Ref. 13)], the bulk doping level (N_D, N_A), and the density and energetic distribution of the surface states. As output the model returns the total tunneling current, the amount of TIBB, and the length over which the potential profile induced by the band-bending extends into the semiconductor crystal.

Some details about the model: Based on a given bias voltage and tip-sample distance, the model constructs the potential profile as a function of the spatial coordinate z by solving the Poisson equation under the constraint that the potential-gradient (electric field) be continuous throughout the region of interest. The resulting potential profile has a trapezoidal shape in the vacuum barrier. To account for effects due to the image charge, the (z-dependent) image potential ''felt'' by an electron between two metal plates is subtracted from the calculated potential in the vacuum barrier. In our model, the image-charge lowers the potential barrier (dotted line in Fig. 3) and thus increases the calculated tunneling current, but does not affect the calculated amount of TIBB. Then the tunneling probability as a function of energy is calculated and integrated over the energy window between the tip and sample Fermi levels. The tunneling matrix element is assumed to vary as a function of energy in the same way as in Ref. 6. The tunneling probability is calculated using the Tersoff-Hamann theory,[14,15] thereby implicitly assuming an s-like tip state. The resulting tunneling current density is multiplied by a fictitious ''tip surface'' which we have set at $10 \times 10\ \mathrm{Å}^2$ to obtain the total tunneling current. For some voltages, part of the tunneling current is generated by electrons tunneling into or out of bulk [bulk valence band (BVB) and bulk conduction band (BCB)] states through a surface depletion layer. The contributions from the BVB states and BCB states are calculated by our model in the same way as in Ref. 6 [see Fig. 3(a)]. The model neglects confinement effects in the accumulation or inversion layer. Furthermore, the model assumes parabolic bands for the bulk states of GaAs in the same way as is done in Ref. 6, with an electron effective mass of 0.067, a light-hole effective mass of 0.09, and a heavy-hole effective mass of 0.45. Finally, the model assumes two bands of surface states (the spatial density is $4.42 \times 10^{14}/\mathrm{cm}^2$). Both bands are 1 eV wide; one extends from the CBM up into the conduction band, and one extends from the valence-bond maximum (VBM) down into the valence band (see figure 3a).

Our model results are in good agreement with the results obtained by in Ref. 6 for TIBB [see Fig. 3(b)]. Only at large voltage (-2.5 and $+2.5$ V) is a deviation from Ref. 6's re-

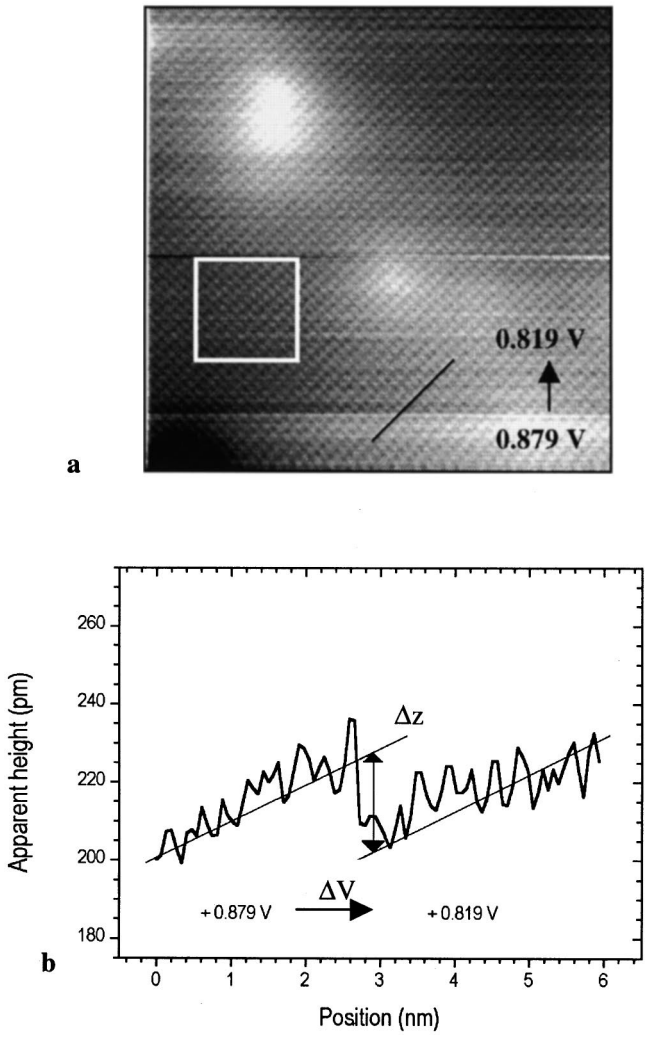

FIG. 4. (a) Typical STM image of n-GaAs: Applied bias voltage: 0.879 V→0.817 V, $I = 254$ pA. Frame size: 20×20 nm, gray scale 0–70 pm. The corrugation numbers and representative frames in Fig. 5 are obtained from cutouts (white rectangle). The horizontal stripes in the image are caused by noise. On the cutout we apply a background correction on each individual (horizontal) scanline. (b): Height-profile taken along [−110] (black line). From the change in apparent height and the voltage difference between the upper and lower parts, $|dz/dV|$ is calculated.

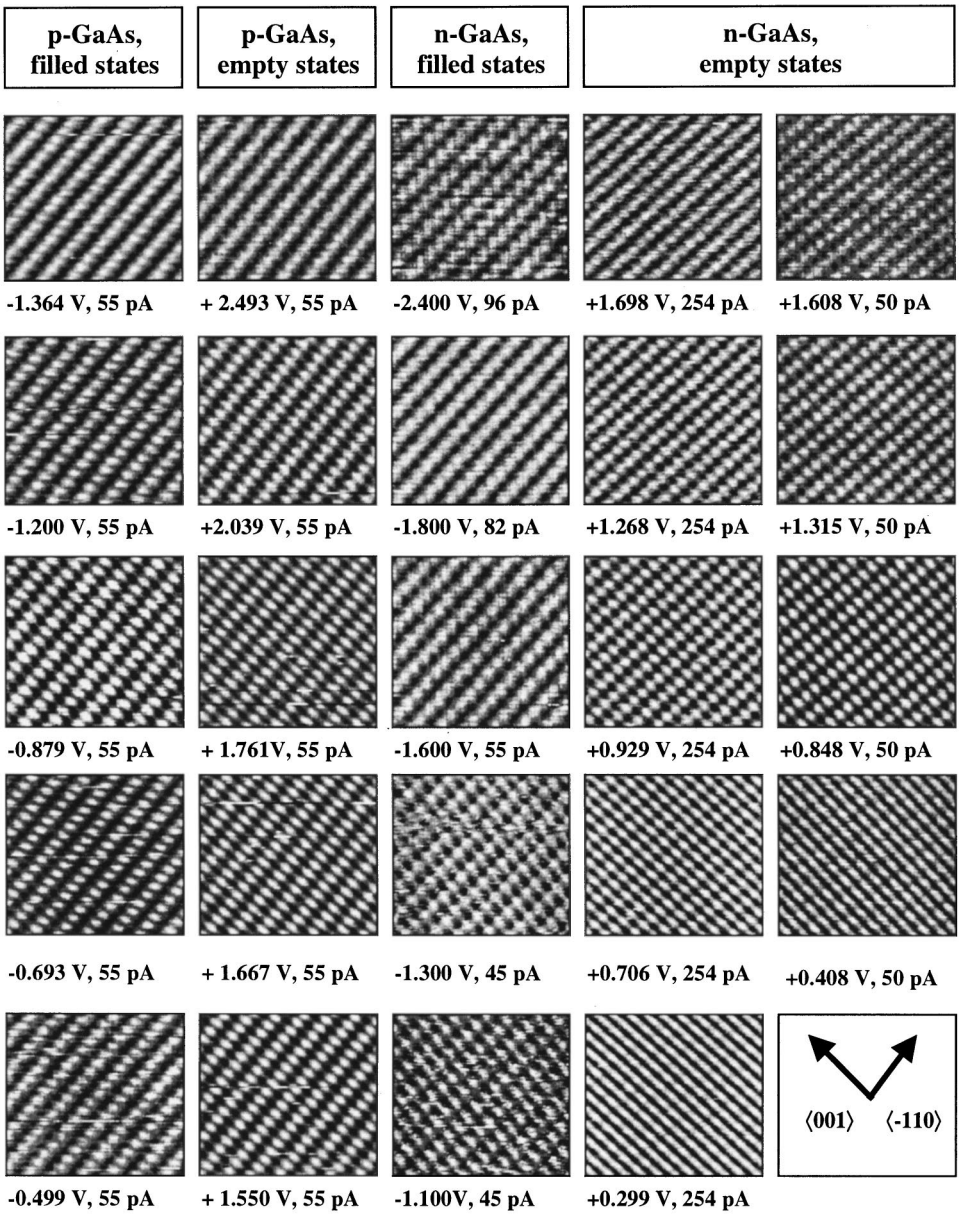

FIG. 5. Voltage-dependent changes in atomic corrugation on GaAs. The frames have been selected from the larger collection of STM frames represented in Fig. 6. Frame size: 5×5 nm. Examples of corrugation number (*n*-GaAs, empty state, $I=254$ pA $V=+1.698$ V; CN$=0.34$; $V=+1.268$ V; CN$=0.19$; $V=+0.929$ V; CN$=0.085$; $V=+0.706$ *V*; CN$=-0.21$; $V=+0.299$: CN$=-0.38$.

sults apparent since our model includes the influence of the two surface-states bands. When these two bands are left out, the model accurately reproduces the results of Ref. 6. Furthermore, we observe that in the limit of small absolute bias voltages, the model sometimes fails to reproduce experimentally observed $I(V)$ points. Instead, the model indicates that no tunneling current can be measured for those parameters. Such events typically involve small tip-sample distance ($z<4$Å) and type-I depletion [see Figs. 7(c) and 8(c)]. We attribute this deviation to the effects of tip-sample interaction, and possibly to a collapse of the tunneling barrier.[16]

When using the model, we adjust the tip-sample distance to reproduce the $I(V)$ points of a given experiment. All other parameters are kept constant. This yields the amount of TIBB as a function of bias voltage for a constant value of the tunneling current. Although the value of the tunneling current used in the simulations is nominally equal to the tunneling current used in the corresponding experiment, we view the value for the tunneling current in the simulations as more or less arbitrary as a real tip usually does not have an *s*-like tip state like the model assumes.[17,18] This whole procedure can be repeated for a different tip work function or tunneling current if the model results appear incompatible with the observed corrugation-changes. The main purpose of the model is to provide insight into the behavior of the amount of TIBB as a function of bias voltage, at constant tunneling current.

III. STM: CORRUGATION CHANGE ON *n*-GaAs(100) AND *p*-GaAs-(110)

We now present voltage-dependent images of *p*-GaAs and *n*-GaAs{110} (Fig. 4), which show clear changes in the apparent direction of the atomic rows as the bias voltage is changed. We have also expressed the changes in terms of the corrugation number (CN) defined in Sec. II (Fig. 6). On

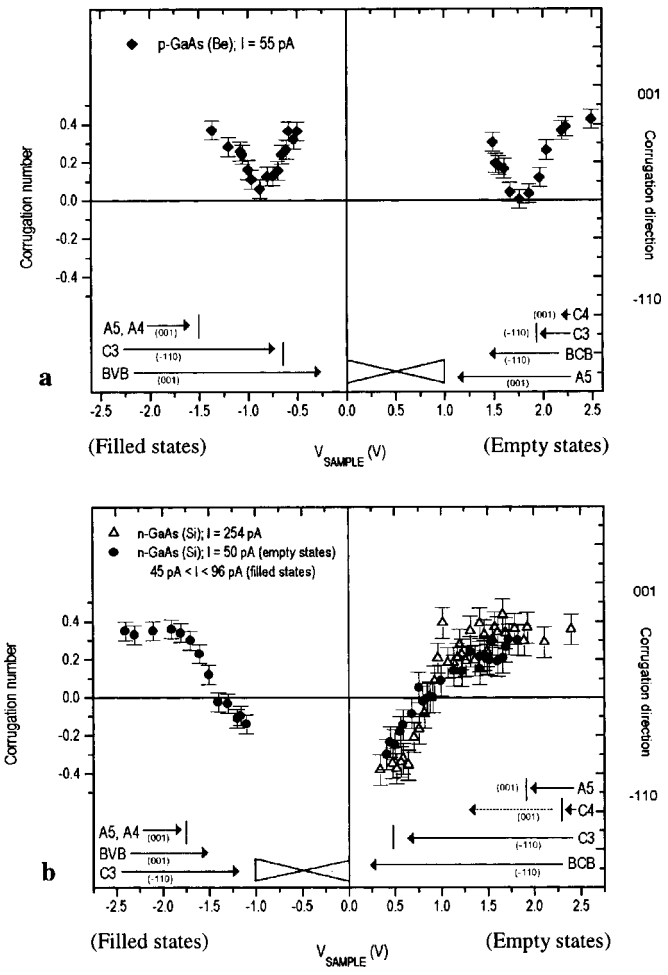

FIG. 6. (a) Corrugation number (CN) for *p*-GaAs. Each point represents one STM frame. The arrows are a schematic representation of the voltage intervals over which we expect contributions from the various surface states. The corrugation direction associated with the state is indicated between parentheses. See further details in Sec. V. (b) CN for *n*-GaAs. The dotted line which is drawn to show the contribution of the $C4$ state (empty states) signifies that at these voltages, we expect the contribution to be from the low-energy shoulder of the $C4$ state (see further details in Sec. V).

p-type material, the corrugation change is only partial: For large bias voltage of either polarity, the corrugation is in the [001] direction. At intermediate voltage, there is a mixed corrugation. This is also reflected by the CN which is close to zero at these voltages. At small voltage, the corrugation is again in the [001] direction, similar to the corrugation observed for large voltage. On *n*-type GaAs there is a complete change in the direction of atomic rows: For large voltage the corrugation is in the [001] direction, and for small voltage it is in the $[-110]$ direction. We have not observed significant differences between the empty states frames obtained at small tunneling current (50 pA), and those acquired using a larger current (254 pA). When using tunneling currents in the range of 50–75 pA, we have repeatedly observed that the resolution gradually deteriorates for $V > +1.5$ V. The reason for this is that as the bias voltage increases, so does the tip-sample distance. With that, the apparent height of the atomic corrugation decreases, until at some point, the corrugation is lost in the background noise. This problem was solved by choosing the larger tunneling current (254 pA).

A special feature of the empty-states results on *n*-GaAs is that we switched from one value for the applied bias voltage to the next one shortly *after* the start of a new frame, rather than between consecutive frames as was done for the other STM images [see Fig. 4(a)] By including the transition from one value of the applied bias voltage to the next, we can observe shifts in the position of the atomic maxima, should these occur. From the changes in the tip-sample distance [see Fig. 4(b)], we can calculate the quantity $|dz/dV|$. We will show later in this paper that the value of $|dz/dV|$ can change dramatically as a function of applied bias voltage, and that from these changes conclusions may be drawn about the amount of TIBB as a function of applied bias voltage.

IV. MODEL RESULTS: DIFFERENT SCENARIOS OF BAND BENDING

Tip-induced band bending (TIBB) is the main factor that determines which of the surface states contributes to the tunneling current at a given bias voltage, and thereby determines the appearance of the atomic corrugation. For this reason we have used our model to calculate the amount of TIBB, given the bias voltages that we applied in our experiments. We have chosen the tip-sample distances in such a way that the total tunneling current calculated by the model equals the currents used in (most of) our measurements. In our discussions, we use an absolute scale for the applied bias voltage (-2 V> -1 V).

The commonly used value of the (average) work function of polycrystalline tungsten is 4.5 eV.[19] However, the different crystal facets of tungsten are known to posess different work functions, varying between 4.3 eV {116} (Refs. 19 and 20) and 5.22 eV {110}.[20] The fabrication process of commercially available polycrystalline tungsten wire can induce a preferential orientation along ⟨110⟩, as a result of the plastic deformations that the wire undergoes while it is thinned down to the right diameter.[11,21,22] This could be a cause for a higher work function than the value used in the model.[11] On the other hand, a contamination near the apex of the tip could well lower the work function. Also, a rough morphology of the surface is known to decrease the work function,[19,23] suggesting that for a tip apex, the work function is inherently reduced. As a working hypothesis, we assume that the work function of our tips usually lies between 4.0 and 4.6 eV (see also Ref. 24).

In Figs. 7 and 8 we show the calculated amount of TIBB for several tip work functions (4.45 and 4.6 eV for *p*-GaAs, and 4.3 and 4.6 eV for *n*-GaAs). Other parameters, such as the tip-sample distance (chosen tunneling current) and the doping concentration also have an influence. However, in the simulations, the influence of the tip work function is much stronger than the influence of the chosen value for the tunneling current. We do not vary the doping concentration in our simulations since the doping concentration of a given sample is usually known in an experiment.[10]

The quantity plotted in Figs. 7 and 8 is the amount of

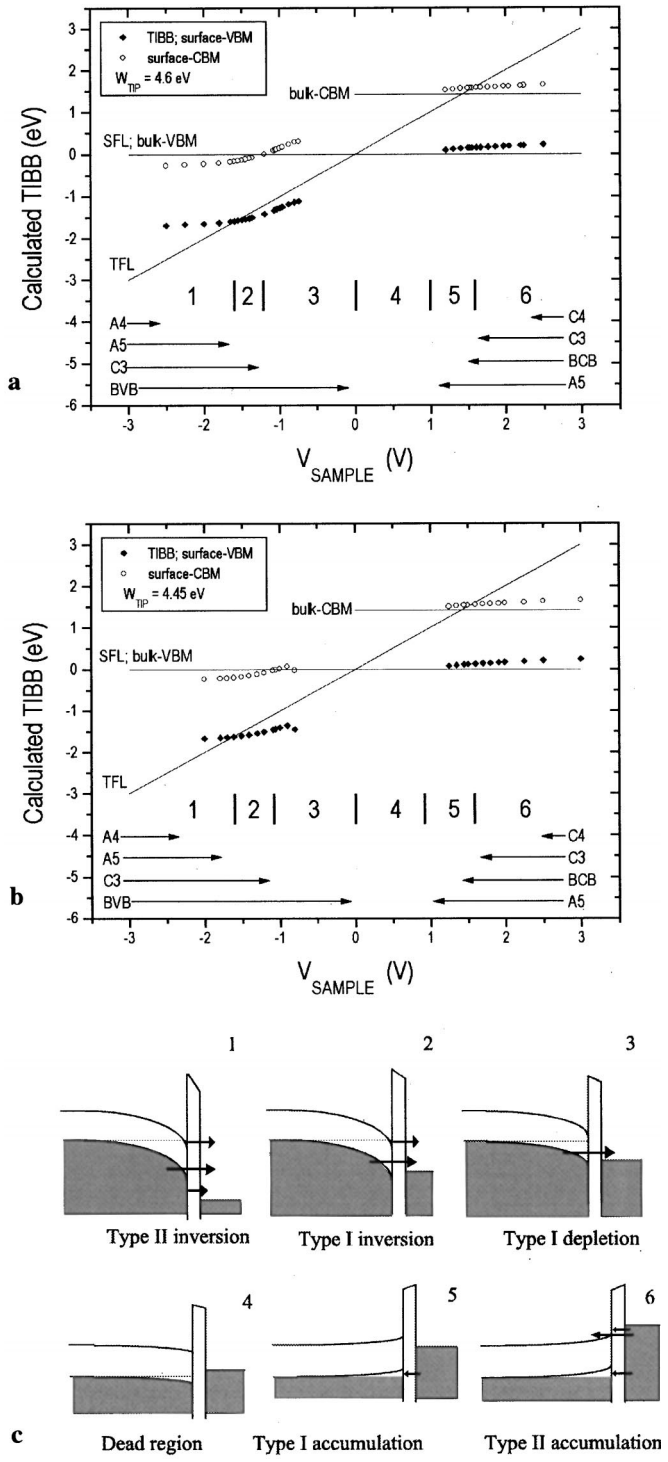

FIG. 7. (a) Tip-induced band bending calculated for *p*-GaAs, $W_{\mathrm{TIP}}=4.6$ eV, $I=55$ pA, and $N_A=10^{18}$ cm^{-3}. The different band bending configurations are indicated by the various numbers. The arrows at the bottom of the plot indicate the voltage-intervals for which we expect a contribution from the different surface and bulk states. (b) TIBB calculated for *p*-GaAs, $W_{\mathrm{TIP}}=4.45$ eV, $I=55$ pA. (c) Different possible band bending configurations on *p*-GaAs.

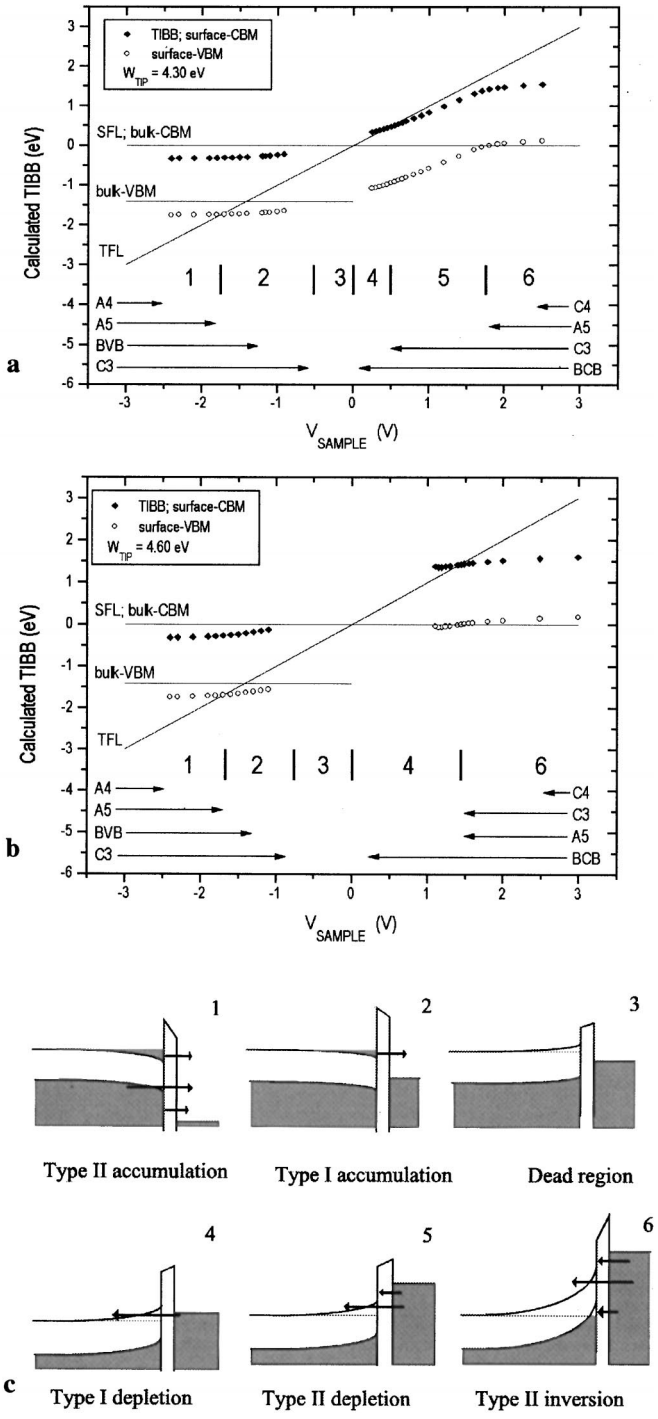

FIG. 8. (a) Tip-induced band bending calculated for *n*-GaAs ($W_{\mathrm{TIP}}=4.3$ eV, $N_D=10^{18}$ cm^{-3}). Simulated currents: 45 pA$<I<$96 pA (filled states), 254 pA (empty states). We have varied the value of the tunneling current in filled states in order to mimick the corresponding measurement. (b) TIBB calculated for *n*-GaAs ($W_{\mathrm{TIP}}=4.6$ eV, $N_D=10^{18}$ cm^{-3}). Simulated currents: 45 pA$<I<$96 pA (filled states), 65 pA (empty states). For these parameters, the model predicts a direct transition from type I depletion to type II inversion. (c) Different possible band bending situations on *n*-GaAs.

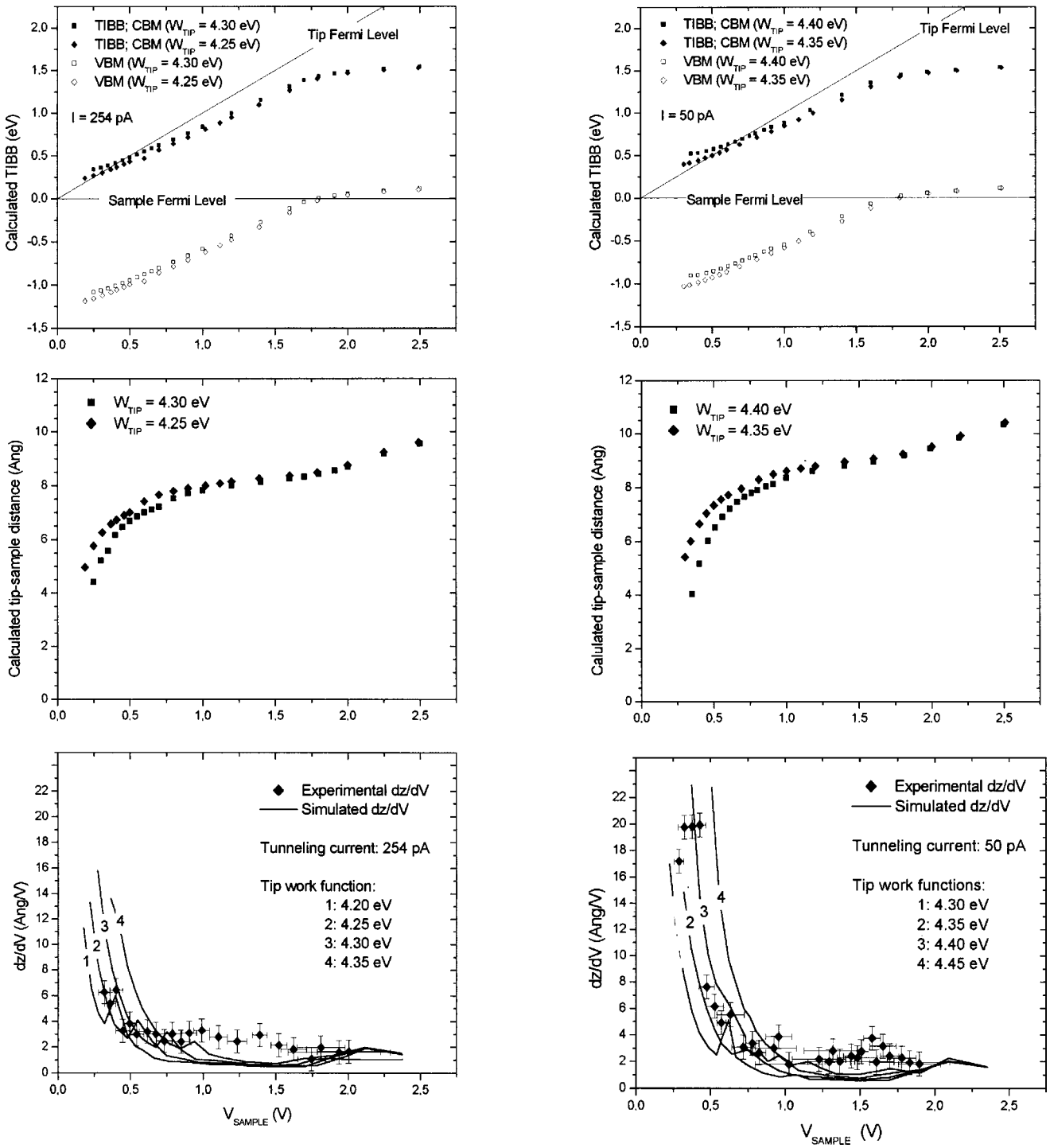

FIG. 9. (a) Calculated TIBB for *n*-GaAs, empty states (see also Fig. 8). For all graphs shown in this figure, the sample voltage is plotted on the horizontal axis [see (c) and (f)]. (b) Tip-sample distance as function of bias voltage $z(V)$. The onset of contributions from the surface states inside the conduction band and the onset of inversion manifest themselves as small discontinuities in the $z(V)$ curves. (c) Comparison between the experimental and calculated dz/dV. For $V<0.5$ V, the sharp decrease in $|dz/dV|$ indicates the transition from type-I depletion to type-II depletion. The left and right ends of the horizontal error-bars correspond to the two voltages between which we switched during the transition. The points are centered on the mean value of the two voltages. The length of the vertical error-bars has been estimated from the noise in the raw STM images. Small peaks appear in the calculated $|dz/dV|$ curves to the small discontinuities in the $z(V)$ curve mentioned in (b). (d) Calculated TIBB for *n*-GaAs, empty states. $I=50$ pA (see also Fig. 7). (e) Tip-sample distance as function of bias voltage $z(V)$. (f) Comparison between the experimental and calculated dz/dV. For $V<0.5$ V, the sharp increase in $|dz/dV|$ indicates the transition from type-I depletion to type-II depletion. The error-bars were estimated in the same way as in (c).

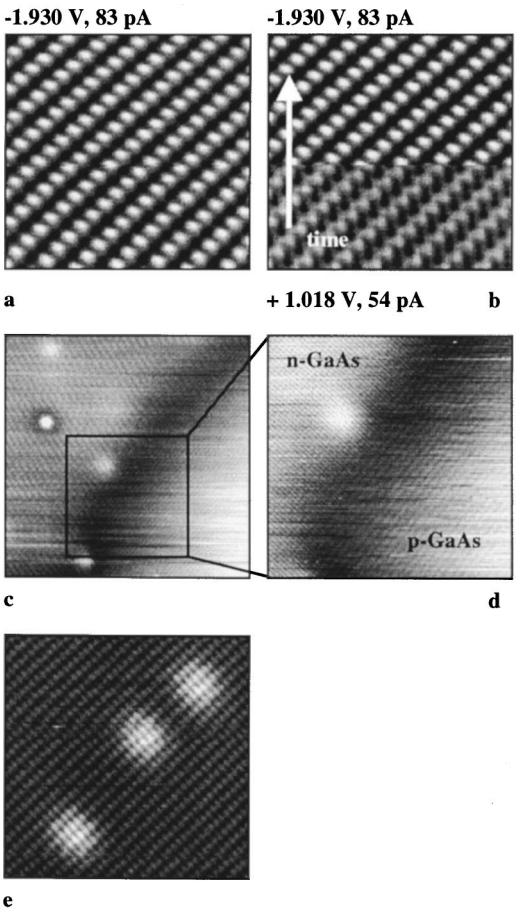

FIG. 10. (a) STM-image of *n*-GaAs in filled states. (b) Same area, for which scanning parameters were switched. The corrugation in the left frame and the upper part of the right frame corresponds to the $A5$ state. The corrugation in the bottom part of the right frame is related to the $C4$ state. Frame size: 5×5 nm. The white arrow indicates the slow scan direction. See further details in text. (c) STM image of a *pn* junction in GaAs. Frame size: 35×35 nm^2, $V=1.698$ V, $I=85$ pA. The depletion region associated with the *pn* junction is visible as a dark band running from the lower left corner of the frame toward the upper right corner. The bright features in the *n*-GaAs part of the frame are Si dopants. (d) The local change in atomic corrugation on either side of a *pn* junction. Frame size: 20×20 nm^2, gray scale: 0–236 pm. (e) Three Si donor atoms which form part of an *n*-type δ-doped layer in GaAs (1×10^{13} cm^{-2}). Near the dopants, the rows appear to run more along (001), as the local positive charge associated with the dopants locally changes the amount of TIBB (see the text). $V=-1.93$ V, $I=96$ Å. Frame size: 11.7×11.7 nm^2. Gray scale: 146 pm.

TIBB relative to the SFL (solid symbols). For *p*-GaAs, the amount of TIBB equals the energetic position of the surface-VBM and for *n*-GaAs it equals that of the surface CBM (see Fig. 3). The surface CBM for *p*-GaAs and the surface VBM for *n*-GaAs have also been indicated (open symbols). We assume that the energetic positions of the surface states remain constant relative to the surface VBM and surface CBM. Consequently, the energetic location of the four surface states is assumed to vary with the applied bias voltage in the same way as the amount of TIBB itself, except for an offset. The band bending plots shown in Figs. 7 and 8 should thus be read in the following way: The part of the surface DOS that falls within the sharp triangle formed between the lines denoting the SFL and TFL lies between the TFL and SFL, and is thus energetically available to the tunneling process. The horizontal arrows indicate the voltage interval over which the electronic states can contribute to the total tunneling current.

p-GaAs

For *p*-GaAs, we identify six different situations, which we label (1) type-II inversion, (2) type-I inversion, (3) type-I depletion, (4) dead region, (5) type-I accumulation, and (6) type-II accumulation. The potential profiles of each of these different situations have been sketched in Fig. 7(c). The significant difference between type-I and II inversion is that in the latter case the (absolute) bias voltage exceeds the amount of TIBB. This allows the valence-band surface states ($A4$ and $A5$) to contribute to the total tunneling current. A similar distinction is made between type-I and II accumulation and depletion.

Several observations can be made from Fig. 7: The first is that for positive sample bias (accumulation), the amount of TIBB remains relatively constant. At negative sample bias, the amount of TIBB is sensitive to the applied bias voltage in the depletion regime and levels off in the inversion regime. Notice that at small negative voltage, there is a voltage-interval for which only the BVB states contribute to the tunneling current. Notice also that the $A5$ and $C3$ states can contribute to the tunneling current at both polarities of the applied sample voltage. This is a direct consequence of TIBB, which can cause these states to be occupied at some voltages and unoccupied at other voltages.

Furthermore, Fig. 7(b) shows that the amount of TIBB can vary nonmonotonically as a function of bias voltage. This is caused by the fact that we maintain a constant value for the tunneling current by adjusting the tip-sample distance in the simulations. At small absolute values of the applied bias voltage, a small change in the bias voltage can cause a relatively large change in the (simulated) tip-sample distance. Where the gradient $d(\mathrm{TIBB})/dV$ is negative [in Fig. 7(b), $-0.9\ \mathrm{V}<V_{\mathrm{bias}}<-0.8\ \mathrm{V}$], the change in the potential gradient between the tip and sample is dominated by the change in the tip-sample distance rather than the change in the applied bias voltage itself. Another point can be seen by comparing Figs. 7(a) and 7(b): A small change in the tip work function can shift the voltage at which the transitions between the different band-bending regimes occur. Consequently, the voltage interval for which any given electronic state can contribute to the tunneling current will depend on the work function of the tip.

Finally, it should be noted that the fraction of the total tunneling current originating from the $C3$ state varies nonmonotonically as a function of bias voltage, with a maximum occurring at some voltage for which the surface is in inversion. This maximum is caused by the changing slope $d(\mathrm{TIBB})/dV$ seen at negative voltage in band bending plots like Figs. 7(a) and 7(b). We can see that the maximum must occur in the following way: When the surface is in type-I

inversion, the total tunneling current consists of a portion from the BVB states and one from the $C3$ state. Near the onset of depletion [at $V=-1.2$ V in Fig. 7(a)], a decrease in the (absolute) bias voltage will decrease the absolute value of TIBB. This, in turn, causes the tunneling current originating from the $C3$ state to decrease as a larger and larger portion of the $C3$ state rises above the SFL where it does not contribute to the tunneling current. The complementary fraction of the tunneling current originating from the BVB states must then increase, as all images are acquired at the same (set point for the) tunneling current. At larger absolute bias where the amount of TIBB levels off [in Fig. 7(a) for $V<-2$ V], increasing the absolute bias voltage will increase the part of the BVB states and the $A5$ state that is available to the tunneling current, whereas the part of the $C3$ state that is available for tunneling remains more or less constant. This also decreases the fraction of the $C3$ state in the total tunneling current. If the fraction of the $C3$ state decreases with decreasing absolute bias voltage at small absolute bias voltage, and also decreases with *increasing* absolute bias at larger absolute bias voltage, it must have a maximum somewhere between.

n-GaAs

For *n*-GaAs, some of the observations to be made are analogous to the ones made for *p*-GaAs: Negative sample voltage involves accumulation whereas depletion and inversion occur at positive sample bias. Also for *n*-GaAs, the amount of TIBB is most sensitive to the applied bias voltage in the depletion regime. Notice that at small positive voltage (type-I depletion), there is a voltage interval for which the electrons can only tunnel into the bulk conduction band (BCB) states. Furthermore, the influence of the tip work function manifests itself quite clearly in the differences between Figs 8(a) and 8(b).

The fact that the band bending behavior in general depends on the tip work function means that finding a meaningful comparison between the simulations and the experiment is not trivial. We can base our interpretation of the experimental results on *p*-GaAs on the images themselves without having to make explicit assumptions about the tip work function, as will be shown in Sec. V. However, the corrugation change in the empty states (positive sample voltage) results on *n*-GaAs is caused by a shifting balance between the contributions of the energetically adjacent $C3$ and $C4$ surface states. The voltage at which the contributions from both states are equally balanced, and thus the voltage for which the corrugation change is observed, critically depends on the work function of the tip used in the experiment.

We can estimate the value for the tip work function to within 0.05 eV from the voltage-dependent changes in the tip-sample distance that we have measured for the empty states results on *n*-GaAs (see Figs. 4 and 9). When calculating the amount of TIBB, the tip-sample distance has to be adjusted for each data point in order to maintain a constant value for the tunneling current. As a result, the calculations also produce a theoretical $z(V)$ curve. Since the absolute tip-sample distance is unknown in a STM experiment, we calculate a theoretical value for $|dz/dV|$ by differentiating the adjacent $z(V)$ points. What is apparent from comparing Figs. 9(a)–9(f) is that the tip-sample distance becomes more sensitive to changes in the applied bias voltage at low voltage, where type-I depletion sets in. This manifests itself in a marked increase of $|dz/dV|$ at the onset of type-I depletion. That same increase at low voltage is also observed in the experimental values of $|dz/dV|$ [Figs. 9(c) and 9(f)]. This indicates that the transition between type-I depletion and type-II depletion occurred for $V\sim+0.5$ V for both the series of images taken at $I=254$ pA (fourth column in Fig. 5) and the series taken at $I=50$ pA (fifth column in Fig. 5). Notice that for both series of images, the band bending behavior involved a large voltage interval of type II depletion.

It may seem problematic to obtain a meaningful comparison between the experimental and theoretical $z(V)$ points for a given measurement. Notice, however, that many of the unknown parameters in the model (such as the tip state) are constant throughout the range of applied bias voltages. Thus a theoretical $z(V)$ curve should at least be proportional to its experimental counterpart, so that voltage-dependent changes in $z(V)$ can still be interpreted meaningfully. Besides, the agreement between the experimental $|dz/dV|$ points and the theoretical $|dz/dV|$ curve indicates that the accuracy of the model is quite reasonable.

A final point to note is that for both *p*-GaAs and *n*-GaAs there are voltage regimes for which (most) of the tunneling current is associated with bulk states, rather than surface states. Feenstra and Stroscio reported that at these voltages, they were not able to obtain meaningful topographic STM results on GaAs ($I=0.1$ nA).[6] In Sec. III we presented voltage-dependent STM-images of clean *n*-GaAs and *p*-GaAs. In Sec. V, we will show that for some of these images, the surface was in type-I depletion with only bulk states contributing to the tunneling current. In spite of that, the images taken at these voltages show a clear atomic corrugation, which in its appearance is not significantly different from the corrugation associated with surface states.

V. DISCUSSION

In this discussion, several questions will be addressed: First we will compare the STM images with the model results concerning TIBB in order to interprete the voltage-dependent changes in atomic corrugation that we have observed. The empty-state results on *p*-GaAs (Sec. V A) and the filled-states results on *n*-GaAs (Sec. V B) are treated first, since these cases involve accumulation and are thus very simple to interpret. Then we will discuss the empty-state results on *n*-GaAs (Sec. V C) and the filled-state results on *p*-GaAs (Sec. V D). In Sec. V D it will be shown that for small, negative sample voltage, the surface of *p*-GaAs is in type-I depletion and the tunneling current originates from the valence-band states in the bulk of the sample (BVB states). For these voltages, atomic corrugation is observed, and Sec. V E theorizes on possible alternative mechanisms for atomic corrugation that might underlie this effect.

A. *p*-GaAs, empty states

The empty-states results of *p*-GaAs [Figs. 5 and 6(a)] show that the atomic corrugation is in the [001] direction at the extrema of the range of applied voltages ($V=+2.5$ and 1.5 V), whereas the corrugation is clearly resolved in both directions for intermediate voltage ($V=+1.8$ V). At $V=+1.5$ V, tunneling occurs mainly into the $A5$ state which has become depopulated by the upward band bending (see Fig. 7). This causes a corrugation in the [001] direction. When the bias voltage is increased, the $C3$ state starts to contribute as well, which is reflected by the reduced CN. When the bias voltage is increased further, the $C4$ state starts to contribute as well, and the corrugation changes back again. Notice that at $V=+1.8$ V, the combined contributions from the $C3$ and $A5$ states reduce the CN down to zero (i.e., there is a partial change in corrugation). This is in contrast to what is observed for *n*-GaAs where the direction of the corrugation changes monotonically from [001] to [−110].

B. *n*-GaAs, filled states

The filled states results on *n*-GaAs [Figs. 5 and 6(b)] show that for high voltage, the corrugation is in the [001] direction. Between $V=-1.8$ and -1.1 V, the corrugation changes from the [001] direction to the [−110] direction. As is evident from Fig. 8, the $C3$ state is populated due to downward band bending at all negative voltages, and thus contributes to the tunneling current at all negative voltages as well. However, between $V=-3$ and -1.8 V the contribution from the $A5$ state dominates the tunneling current and the corrugation is in the [001] direction. Only at a small negative voltage where the $C3$ state is the main contributor to the tunneling current is the corrugation in the [−110] direction.

C. *n*-GaAs, empty states

The empty-state images of *n*-GaAs show a gradual corrugation change as is shown in Figs. 5 and 6(b). In the recorded transitions between the applied voltages we have not observed any shifts in the atomic rows [see Figs. 10(a) and 10(b) for an example of such a shift]. This indicates that the atomic maxima represent the top row Ga atoms for all positive bias voltages. Consequently, we can attribute the corrugation-change in the empty-state images of *n*-GaAs to a shifting balance between the competing contributions of the $C3$ and $C4$ states.

The point at which the CN changes sign lies near $V=+0.9$ V for both measurements (i.e., $I=50$ and 254 pA). According to the model calculations the TFL lies between 0 and 0.2 eV above the surface CBM for that voltage. The model thus indicates that the TFL lies below the nominal energetic positions of both the $C3$ and $C4$ states[3] when the actual corrugation change occurs, instead of between the nominal energetic positions of these two states which one might intuitively expect. Given the agreement between the calculated and experimental values for $|dz/dV|$, (see Fig. 9) we are convinced that the model calculations describe the band bending behavior correctly, at least in qualitative terms. Moreover, the slow rise of the TFL with respect to the surface CBM predicted in the model is also consistent with the experimental observation that the corrugation changes quite gradually as a function of applied bias voltage. We offer the following hypothesis as a possible explanation for this result: From the calculated surface DOS on InP {110} (see Fig. 1 in Ref. 1), the $C3$ state appears as a small peak superimposed on some background. If the low energy shoulder of the $C4$ state forms a background on which the DOS associated with the $C3$ state is superimposed, the $C4$ state might influence the corrugation even when tunneling occurs at energies below the nominal energetic position of the lower-lying $C3$ state.

Notice that according to Figs. 8 and 9, the sample surface was in type-I depletion for $V<0.5$ V. This band bending situation involves electrons tunneling from the tip into the bulk states of the conduction band through a surface depletion layer. At the same time, we observe for these voltages a corrugation with the atomic rows running along [001]. We attribute this corrugation to the low-energy shoulder of the $C3$ state, which is reported to extend into the band gap.[3,4]

D. *p*-GaAs, filled states

The filled-state results obtained on *p*-GaAs shown in Figs. 5 and 6 show that at large negative voltage, the atomic corrugation is in the [001] direction. A mixed corrugation appears at intermediate voltage ($V=-0.9$ V), and at low voltage ($V=-0.5$ V) the corrugation is again in the [001] direction. As we lack experimental dz/dV data for the results on *p*-GaAs, we have to base our analysis entirely on the corrugation direction observed in the images. The observed changes in atomic corrugation can be explained in a very straightforward manner if one accepts the following hypothesis: the contribution of the BVB states is spatially modulated so as to produce an atomic-like corrugation in the [001] direction (see Fig. 5: *p*-GaAs, $V=-0.499$ V).

Let us start by considering the minimum in the CN that occurs for $V=-0.9$ V. This partial change in corrugation indicates that the $C3$ state is populated and contributes to the total tunneling current, since the $C3$ state is the only surface state that causes an atomic corrugation in the [−110] direction. On *p*-GaAs, the $C3$ state can only become populated when the surface is in inversion. At the same time, it is clear from the fact that a mixed corrugation is observed that there must be a second contribution from an other state which causes a corrugation in the [001] direction. Together, the two contributions cause a mixed corrugation to appear in the image. At first sight the logical interpretation would be that the mixed corrugation is caused by the combined contributions of the $A5$ state and the $C3$ state, assuming that the latter has become populated by inversion.

However, it becomes clear that this interpretation must be wrong when the voltage at which the mixed corrugation occurs, is considered: If the $C3$ state is to contribute to the filled-states tunneling current, it must lie energetically below the sample Fermi level (SFL). The fact that the $C3$ state lies energetically near the SFL implies that the $A5$ and $A4$ states must lie well below the tip Fermi level (TFL) and thus cannot contribute to the total tunneling current. The reason for

this is that the bias voltage at which the mixed corrugation occurs ($V=-0.9$ V), is less than the energetic separation of the $A5$ and $C3$ states, which lie on either side of the band gap ($E_g=1.42$ eV).[13] Thus the surface must be in type-I inversion. From Fig. 7 we now identify the BVB states as the origin of the second contribution to the total tunneling current at $V=-0.9$ V. In order to explain the fact that we observe a mixed corrugation at this voltage, we have to assume that the contribution from the BVB states is associated with an atomic-like corrugation in the [001] direction.

When the voltage increases from $V=-0.9$ to -1.4 V, the increase in the CN [see Figs. 5 and 6(a)] is attributed to an increased relative contribution of the BVB states: As the negative voltage increases, the contribution from the BVB states increases whereas the contribution from the $C3$ state remains more or less constant. This is caused by the amount of TIBB leveling off at the onset of inversion (see Fig. 7). We can exclude any contribution from the $A5$ state for this voltage region because the absolute value of the bias voltage remains less than 1.4 V. When the voltage is decreased from $V=-0.9$ to -0.5 V, the CN rises as well [see Fig. 6(a)]. We attribute this rise in CN to an increased relative influence from the BVB states: Figure 7 shows that as the voltage decreases from $V=-0.9$ to -0.5 V, the contribution from the $C3$ state vanishes and the one from the BVB states remains. We ignore the non-monotonous behavior shown in Fig. 7(b) for the moment as we do not observe any signs of such nonmonotonic band bending in our STM images (Figs. 5 and 6). The change in corrugation could in principle also be explained from an increased contribution from the $A5$ state, although a contribution of the $A5$ state at $V=-0.5$ V would imply a band bending behavior that is inconsistent with our band bending model.

There are a few additional remarks to be made. First of all, we neglect any possible involvement of the low-energy tail[4] of the $C3$ state (see Sec. I), for two reasons. From Ref. 3 it is clear that the energetic part of the surface DOS associated with the tail decays very rapidly into the vacuum. At a simulated tip-sample distance of 3.3Å, it does not significantly contribute to the local surface DOS.[3] From our model results, we do not expect the tip-sample separation to become less than about 4Å, therefore, we do not think this part of the surface DOS contributes significantly to the tunneling current at the tip-sample separations typical for our experiments. The second reason is that the fraction of the tunneling current originating from the C3 state evidently maximizes around $V=-0.9$ V, indicating that for this voltage the surface must be in inversion (see Sec. IV).

A very compelling argument in support of our theory is that we have based our interpretation on a band bending behavior that is consistent with the results presented by Feenstra and Stroscio.[6] In that paper, the authors compare experimental $I(V)$ spectra of GaAs (110) with model calculations. The model very specifically considers the effects of electrons tunneling into or out of bulk states through a surface depletion layer caused by TIBB. The authors find that the experimental results can only be reproduced by the model if the current generated by electrons tunneling through a surface depletion layer into or out of bulk states, is included. It is thus clear that it is very well possible to obtain a measurable tunneling current from electrons tunneling out of bulk states through a surface depletion zone. In fact, the phenomenon seems a very common occurrence from Ref. 6. When this band bending behavior is combined with the assumption that a contribution from the BVB states is somehow associated with atomic-like corrugation in the [001] direction, the explanation of our own experimental results follows in a very straightforward and natural way.

The last remark is that we cannot find a reasonable explanation for our experimental results under the assumption that atomic corrugation can only be caused by electrons tunneling directly into or out of surface states. The mixed corrugation occurring at $V=-0.9$ V cannot be caused by a combined contribution from the $A5$ (or $A4$) state and the $C3$ state, as these states lie energetically too far apart. That would leave the $C4$ state as the remaining state that might cause a corrugation in the [001] direction. In our model we find that it is possible to populate the conduction band by inversion to up to about 0.2 eV. It is unclear to us whether that is sufficient to expect a corrugation in the [001] direction from the $C4$ state, but in view of our empty-state results on n-GaAs we will assume for the moment that it is. However, we cannot find a set of parameters that gives a voltage-dependent behavior of TIBB that would be consistent with the observed corrugation changes. Most importantly, the model indicates that there must be a voltage region for which the $C3$-state dominates the tunneling current. This would cause a corrugation in the [−110] direction (a CN less than 0), which is clearly not observed for p-GaAs.

E. Atomic corrugation while tunneling out of bulk states

In Sec. V D we concluded that the contribution from the BVB states has to be associated with an atomic corrugation in the [001] direction. In this subsection, we will reflect on possible mechanisms for such corrugation. It is in any case clear that the corrugation observed in the type-I depletion regime must be associated with the surface of the crystal. At the surface, there is a clear distinction between the top row As sites and the bottom row As sites [Fig. 1(b)]. Inside the crystal, the As atoms located on a [110] axis below a top row As surface atom are equivalent to the As located below a bottom row As surface atom. If the inside of the crystal (more specifically, the spatial distribution of the valence band charge in the bulk) could be imaged by electrons tunneling through the depletion layer, this would manifest itself as a doubling of the periodicity in the observed lattice. In Fig. 5 no such doubling of the periodicity is observed.

One possible mechanism is that the corrugation is caused by atomic-scale variations of the tunneling barrier-height. Such variations have been observed experimentally for different reconstructions of the Si(111) surface and for the $2\times n$ reconstruction of Si(001).[8,9] Another possibility is that the atomic corrugation associated with the tunneling current from the BVB states is the result of a site-dependent tip-sample interaction. When the tip shank relaxes under the varying tip-sample interaction, this might cause the tip apex to move alternatingly toward or away from the sample sur-

face as the tip is scanned. The resulting modulation in the tunneling current (or in the measured tip height for constant current STM) would then reflect the local variations of the tip-sample interaction itself. Our band bending model indicates tip-sample distances of (4–7) Å during tunneling while the surface is in type-I depletion. In this regime of tip-sample distance, the tip-sample interaction is dominated by the *resonance interaction*,[15] which is attractive and site dependent. Unlike the tunneling current, which exists between two spatially overlapping states that have the same energy, the attractive force caused by the resonance interaction also exists between two spatially overlapping states of different energies.[15,25] Notice that the expected range of tip-sample distances [(4–7) Å] is outside the region of chemical bond formation in the way described by Ke *et al.*[26] The GaAs {110} surface has dangling-bond states associated with both the As atoms and the Ga atoms; therefore one might intuitively suspect that an image based on the local variations of the tip-sample interaction would show both atom-species at the same time. However, recent scanning force microscopy images of *n*-type InAs {110} presented by Schwarz *et al.* show only the As sublattice,[27] so the assumption of a corrugation mechanism in STM based on the tip-sample interaction forces that only shows one of the atom species (probably As), seems quite reasonable.

Obviously the above considerations are not conclusive. However, it is in any case clear that experimental circumstances exist for which the electrons making up the tunneling current cannot tunnel directly into or out of surface states. In spite of that, atomic, surfacelike corrugation is observed for these circumstances. Apparently there are alternative mechanisms for atomic corrugation in STM images of GaAs {110} that manifest themselves under the appropriate experimental conditions. Therefore, the common view of atomic resolution in STM images of semiconductor surfaces, that involves electrons tunneling directly into or out of surface states, can no longer be regarded as complete.

VI. SOME OTHER EXAMPLES OF CORRUGATION CHANGE ON GaAs(110)

Over the course of our experiments, some of which are not directly related to the work presented in this paper, we have observed corrugation changes many times. In this section, we show three illustrative examples.

The first example shows the transition from filled states imaging to empty states imaging on an *n*-GaAs substrate. For this measurement, we operated the STM in a ''dual mode.'' The scanning voltages are shown in Figs. 10(a) and 10(b). As the frame was recorded, we changed the scanning parameters for the backward frame from $V=+1.018$ V, 54 pA to $V=-1.930$ V, 83 pA. Consequently, the bottom part of Fig. 10(b) shows the lateral distribution of $C4$ state whereas the top part of Fig. 10(b) shows the $A5$ state. Notice the lateral shift in the position of the atomic maxima. The parameters for the forward scan remained unchanged. The forward scan, which remains unchanged, shows that the tip DOS remained the same during the voltage change in the backward scan.

The second example that we show is the corrugation change around a *p-n* junction. This junction was formed by a Be δ layer (1×10^{13} cm^{-2}) and an *n*-doped cap layer (Si : 4×10^{18} cm^{-3}) that was grown on top of it. The δ layer was overgrown by 27 nm of nonintentionally doped GaAs and then by *n*-type GaAs. Somewhere between the Be δ layer and the cap layer, a *p-n* junction formed which we recognized in our image from the depletion zone that is associated with such a junction [Fig. 10(c)]. The bright spot near the depletion zone is a Si dopant. The image was obtained at $V=-1.698$ V, 85 pA. The *n*-GaAs portion of the image shows rows running along [001] whereas the *p*-GaAs portion shows rows running along [−110]. Due to the downward band bending, the *n*-GaAs portion of the surface is in accumulation. This populates the $C3$ state and causes the atomic rows to run along [001]. For the *p*-type portion of the surface, we expect contributions from the BVB states and the $A5$ state, causing the atomic rows to run along [−110].

Finally, we show the local corrugation change associated with subsurface Si dopants[28] [Fig. 10(e)]. The image shows part of a Si δ-doped layer (1×10^{13} cm^{-2}) in GaAs. The applied bias voltage was $V=-1.93$ V, and the tunneling current was 96 pA. For these conditions, the donor atoms are neutral since the surface is in accumulation. However, within the Bohr radius of the bound electron, the positive charge of the Si impurity is no longer screened completely. This positive charge will locally decrease the potential for electrons, resulting in a local increase of the downward band bending. That increases the contribution from the $C3$ state relative to the ones from the BVB states and the $A5$ state, which manifests itself as a change in corrugation near the dopant atoms.

VII. SUMMARY AND CONCLUSIONS

In this paper, we have analyzed voltage-dependent images of the GaAs{110} surface while considering calculated values for tip-induced band bending obtained from a one-dimensional model. For the empty-state results on *n*-GaAs we have validated the model by comparing measured and theoretical values for $|dz/dV|$ as a function of applied bias voltage. Furthermore, for both *p*-GaAs and *n*-GaAs a voltage regime exists for which none of surface states can contribute to the tunneling current (type-I depletion). In spite of that, atomic, surfacelike corrugation is observed in this voltage regime, both on *p*-GaAs and on *n*-GaAs. The mechanisms underlying this corrugations are as yet unclear. In the case of *n*-GaAs, we attribute the observed corrugation to the influence of the low-energy shoulder of the $C3$ state, which is known to extend into the band gap. In any case, the corrugation observed for the type-I depletion regime cannot be explained by electrons tunneling directly into or out of surface states, which is the common way to understand atomic resolution on semiconductor surfaces. This work shows that there must be alternative mechanisms for atomic corrugation in STM images that manifest themselves under certain experimental conditions. Understanding the mechanisms by which atomic corrugation might occur in the band bending regime of type-I depletion is a clear challenge and an exiting prospect for future research.

ACKNOWLEDGMENTS

We gratefully acknowledge stimulating discussions with J. Frenken, M. Wenderoth and J. W. v.d. Horst. We also thank V. G. Mokerov and A. P. Senichkin of the Institute of Radioengeneering and Electronics, Russian Academy of Sciences, Moscow, for the growth of the material shown in Fig. 10(c) and 10(d). This work was part of the research program of the ''Stichting voor Fundamenteel Onderzoek der Materie (FOM),'' which was financially supported by the ''Nederlandse Organisatie voor Wetenschappelijk Onderzoek (NWO).''

[1] Ph. Ebert, B. Engels, P. Richard, K. Schroeder, S. Blügel, C. Domke, M. Heinrich, and K. Urban, Phys. Rev. Lett. **77**, 2997 (1996).

[2] J. R. Chelikowski and M. L. Cohen, Phys. Rev. B **20**, 4150 (1979).

[3] B. Engels, P. Richard, K. Schroeder, S. Blügel, Ph. Ebert, and K. Urban, Phys. Rev. B **58**, 7799 (1998).

[4] J. R. Chelikowski, S. G. Louie, and M. L. Cohen, Phys. Rev. B **14**, 4724 (1976).

[5] C. S. Jiang, T. Nakayama, and M. Aono, Jpn. J. Appl. Phys. **36**, L1336 (1997).

[6] R. M. Feenstra and J. A. Stroscio, J. Vac. Sci. Technol. B **5**, 923 (1987).

[7] N. D. Jäger, E. R. Weber, and M. Salmeron, J. Vac. Sci. Technol. B **19**, 511 (2001).

[8] N. Horiguchi, K. Yonei, and M. Miyano, Jpn. J. Appl. Phys. **37**, 3782 (1998).

[9] H. Fukumizu, S. Kurokawa, A. Sakai, and Y. Hasegawa, Jpn. J. Appl. Phys. **37**, 3785 (1998).

[10] We use commercially available *n*-doped GaAs wafers with a nominal doping concentration of 1×10^{18} cm^{-3}. The actual doping concentration may lie between 1 and 2×10^{18} cm^{-3}.

[11] G. J. de Raad, P. M. Koenraad, and J. H. Wolter, J. Vac. Sci. Technol. B **17**, 1946 (1999).

[12] G. J. de Raad, D. M. Bruls, P. M. Koenraad, and J. H. Wolter, Phys. Rev. B **64**, 075314 (2001).

[13] E. F. Schubert, *Doping in III–V Semiconductors*, (Cambridge University Press, Cambridge, 1993), p. 541.

[14] J. Tersoff and D. R. Hamann, Phys. Rev. Lett. **50**, 1998 (1983); Phys. Rev. B **31**, 805 (1985).

[15] C. J. Chen, *Introduction to Scanning Tunneling Microscopy*, (Oxford University Press, Oxford, 1993). Chap. 3 explains that for an *s*-like tip state, the tunneling matrix element is proportional to the surface density of states of the sample evaluated at the centre of the tip apex atom. The tip-sample interaction effects relevant for this paper are explained on p. 177 and further, and on p. 189.

[16] S. Ciraci in *Scanning Tunneling Microscopy III*, edited by R. Wiesendanger and H. J. Günteroth, Springer Verlag Berlin, p. 182, p. 197 (1996).

[17] S. Ohnishi and M. Tsukada, Solid State Commun. **71**, 391 (1989).

[18] M. Tsukada, K. Kobayashi, and S. Ohnishi, J. Vac. Sci. Technol. A **8**, 160 (1990).

[19] W. P. Dyke and W. W. Dolan, in *Advances in Electronics and Electron Physics* (Academic, New York, 1956), Vol. VIII, pp. 89–185, especially p. 114.

[20] *CRC Handbook of Chemistry and Physics*, 60th ed. (CRC Press, Boca Raton, FL, 1980), p. E-83.

[21] R. Gomer, *Field Emission and Ionization*, (Harvard University Press, Cambridge, MA, 1961), p. 45.

[22] S. W. H. Yih and T. Wang, *Tungsten: Sources, Metallurgy, Properties and Application* (Plenum, New York, 1979), pp. 209–222.

[23] R. Smoluchowski, Phys. Rev. **60**, 661 (1941).

[24] R. Dombrowski, Chr. Steinebach, Chr. Wittneven, M. Morgenstern, and R. Wiesendanger, Phys. Rev. B **59**, 8043 (1999).

[25] R. L. DeKock and H. B. Gray, *Chemical Structure and Bonding*, (Benjamin/Cummings, Menlo Park, CA, 1980), pp. 193 and 253.

[26] S. H. Ke, T. Uda, R. Perez, I. Stich, and K. Terakura, Phys. Rev. B **60**, 11 639 (1999).

[27] A. Schwarz, W. Allers, U. D. Schwarz, and R. Wiesendanger, Phys. Rev. B **61**, 2837 (2000).

[28] C. Domke, M. Heinrich, Ph. Ebert, and K. Urban, J. Vac. Sci. Technol. B **16**, 2825 (1998).